

NASA Contractor Report 4209

Optical Backplane Interconnect Technology (OBIT)

J. M. Hammer
David Sarnoff Research Center
Princeton, New Jersey

Prepared for
Langley Research Center
under Contract NAS1-18226



National Aeronautics
and Space Administration

Scientific and Technical
Information Division

1988

Table of Contents

Section		Page
I.	INTRODUCTION	I-1
II.	GRATING-SURFACE-EMITTING WAVEGUIDE, TUNABLE-LASER (GSE-TL) APPROACH	II-1
III.	METHODS OF SCANNING GSE OPTICAL BEAMS	III-1
	A. Resolution of Angularly Scanned Optical Beams	III-1
	B. Beam Scanning Possibilities with GSE Waveguides	III-2
IV.	WAVELENGTH TUNING RANGE AND RESOLUTION OF GSE-TL APPROACH	IV-1
	A. Resolution of Wavelength Scanned GSE	IV-1
	B. Tuning Abrupt DSR Grating Requirements	IV-3
V.	POWER REQUIREMENTS AND LOSSES	V-1
	A. Receiver Power Needed to Achieve 10^{-9} BER	V-1
	B. System Losses	V-2
	C. Summary of Optical Losses	V-9
VI.	CONCLUSIONS	VI-1
VII.	REFERENCES	VII-1
APPENDIX		

PRECEDING PAGE BLANK NOT FILMED

List of Illustrations

Figure		Page
II-1	Schematic of monolithic grating-surface-emitting waveguide tunable-laser (GSE-TL) array approach to optical backplane interconnect technology (OBIT).	II-2
II-2	Detail of GSE-TL OBIT approach.	II-3
II-3	Schematic of lenticular lens array of focal length f positioned to couple two GSE-TL arrays together to form a complete backplane interconnect for computer use. The focal length of the lenslets in the lenticular array may be chosen to optimize the optical coupling between the arrays.	II-3
III-1	Illustration of diffraction spreading from aperture.	III-1
III-2	Illustration of how diffraction effects number of resolved spots.	III-2
III-3	Schematic of grating surface emitting (GSE) waveguide.	III-2
IV-1	Effective aperture, D_e , is less than the aperture D when Θ is not 90°	IV-1
IV-2	Number of addressable rows plotted against the output coupling angle measured from the normal to the waveguide plane when the the wavelength is tuned $\pm 100 \text{ \AA}$ around a center value of $0.83 \mu\text{m}$. The GSE waveguide grating length $D = 500 \mu\text{m}$, $n_e = 3.4$, and $n_0 = 1$	IV-3
IV-3	Cross-section through a GSE waveguide. The refractive index of the waveguide layer is $n_f = 3.48$. That of the substrate is $n_s = 3.39$. The cover is assumed to be air with a refractive index $n_c = 1$	IV-4

**List of Illustrations
(cont'd.)**

Figure		Page
IV-4	Plot of Bragg reflecting grating length (left ordinate) and grating reflection line width $\Delta\lambda$ (right ordinate) against grating reflectivity for a grating on an AlGaAs waveguide. The strong grating has a depth g of $0.1 \mu\text{m}$, which is 25% of the guide thickness.	IV-6
V-1	Equivalent circuit representation of unit cell of OBIT array operated in the receiving mode.	V-1
V-2	Directional coupler consisting of two identical rectangular dielectric waveguides of refractive index n_f embedded in a substrate of lower refractive index n_s	V-4
V-3	Variation of transmission from waveguide to GSE grating with directional coupler number for $\delta\lambda = 200 \text{ \AA}$	V-5
V-4	Perspective view of geometry for calculating coupling between two GSE-TL arrays.....	V-9

Section I

INTRODUCTION

We have proposed and analyzed a novel approach for implementing an optical back plane interconnect technology (OBIT) that is capable of optically connecting any row of a 32 x 32 backplane array to any row of a second 32 x 32 array. Each backplane array is formed monolithically on a wafer. The technology is based on the use of grating-surface-emitting (GSE) waveguides that are formed on a wafer containing a quantum well and a separate confinement waveguide. The quantum well and waveguide serve a number of functions being used for transverse guiding, gain, modulation, detection, and the formation of a wavelength-tunable distributed-Bragg reflector laser. Photolithographically formed ridges and electrode structures provide lateral guiding and the control of the required light generation, modulation, and detection functions. The GSE waveguides act as efficient antennae that radiate light at an angle selected by tuning the wavelength of the lasers from the transmitting array to the receiving array. The same waveguides may be used as the receiving antennae when the array is used in the receiving mode. Thus, wavelength tuning is used to direct each row of the transmitting array to the desired row of the receiving array. It is also possible to include separate transmitting and receiving structures on the same monolithic array to allow duplex operation. We have, however, not treated this case in detail.

We may summarize the results of our study as follows: Using our approach, which is outlined above and described in greater detail in the body of this report, it should be possible, within the present state of the art, to have an optical backplane array with the following characteristics:

- Any row of a 32 x 32 GSE array may be optically connected to any row of a second 32 x 32 array.
- By scanning the laser driver of a row of the transmitting array through a wavelength range of 200 Å, any of 32 rows of the receiving array can be addressed.

- Each monolithic array can be used as both transmitter and receiver by switching the bias on the quantum-well switch-detectors.
- Separate transmitting and receiving structures could be provided, if desired, for duplex operation.
- For a bit error rate of 10^{-9} at a 100 MHz data rate, a required laser power of 12 mW is calculated based on an estimated total optical loss of 40 dB (9.7×10^{-5}).

The advantages of this approach to OBIT are as follows:

- Provides an optical approach to overcome complexity inherent in electronic switching for computer applications.
- Employs and monolithically integrates waveguide and laser diode devices that have been demonstrated. It thus does not require the invention of new devices.
- Because a complete backplane array may be formed monolithically on a chip, our approach will be compact and power efficient.
- It should be possible to demonstrate optical backplane switches, as large as 32 x 32, using state-of-the-art technology.
- The optical backplane technology studied in this report requires only one switch decision, to switch 32 parallel connections to any one of 32 positions.
- The laser power required to achieve a high level of performance (32 parallel connections to any of 32 positions with 10^{-9} BER at a 100-MHz data rate) is modest for certain types of quantum-well lasers.

Section II

GRATING-SURFACE-EMITTING WAVEGUIDE, TUNABLE-LASER (GSE-TL) APPROACH

In this section we will describe the approach used as the model for the major part of this study. The detailed descriptions and analysis required to evaluate the feasibility of the approach will be given in Sections IV and V. Some general considerations that bear on the scanning of light beams are discussed in Section III.

The grating-surface-emitting waveguide, tunable-laser (GSE-TL) approach is shown in Figs. II-1, II-2, and II-3. The illustrated array can be used as either an optical transmitter or an optical receiver of coded information. The GSE-TL approach may be described as a monolithic array of grating-surface-emitting (GSE) waveguides connected to abrupt DBR tunable lasers through integrated waveguide directional couplers and combined quantum-well switch-detector sections.

We envisage a quantum-well-waveguide (QWWG) and other epitaxial layers as being grown over the entire wafer. The laser, switch, amplifier, and ridge structures that guide waves in the desired directions in the plane of the QWWG are then formed using photolithographic processes as required. The gratings may be formed by holographic exposure and etching at a suitable stage during the processing. Electrodes may also be deposited at the appropriate processing stage.

The array operates as an optical transmitter as follows: Light from each of the abrupt DBR tunable lasers connected at the left of each row is distributed equally to the each of the GSE waveguides in the row. The wavelength of the light in a particular row can be adjusted independently of the wavelength of other rows by setting the currents in the laser pump and tuning buses feeding that row. The light is emitted out of the GSE waveguide plane (the y-z plane) by the grating that acts as an output coupler [1]. Light emerges at an angle Θ_i to the x axis in the x-y plane. Θ_i depends on the light wavelength (λ) and the period of the grating (Λ). Thus each row of the transmitting array can be independently addressed to a desired row of the receiving array by tuning the laser driving that row. This says that only one switch decision is required to connect all the cells of one row to the corresponding cells of the receiving row.

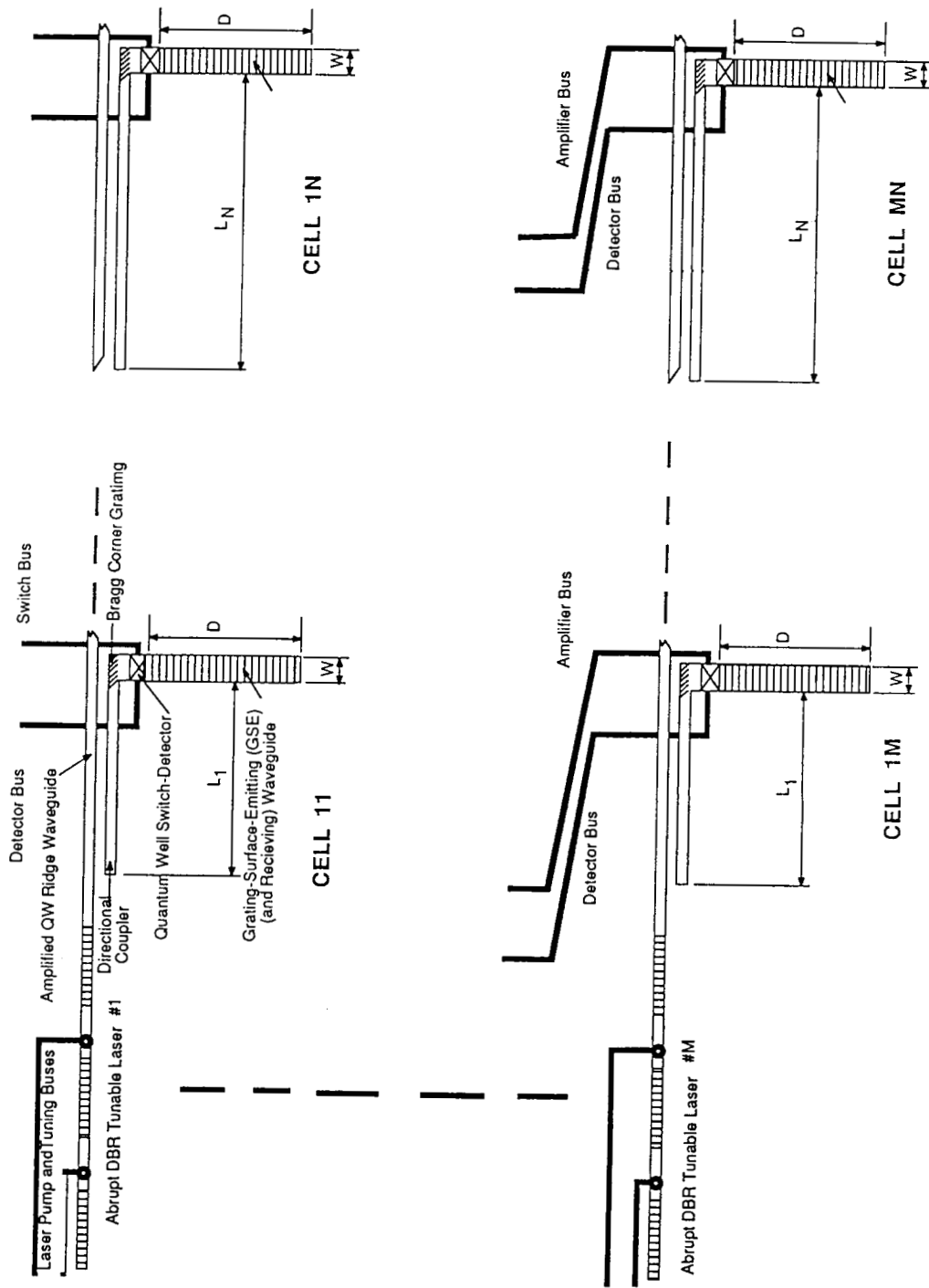


Figure II-1. Schematic of monolithic grating-surface-emitting waveguide tunable-laser (GSE-TL) array approach to optical backplane interconnect technology (OBT).

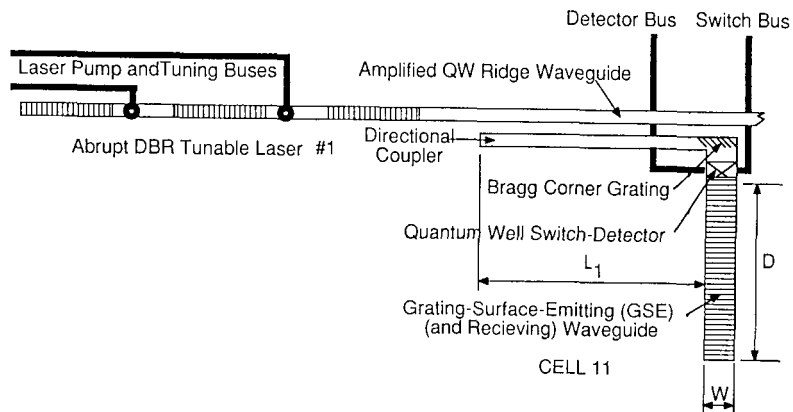


Figure II-2. Detail of GSE-TL OBIT approach.

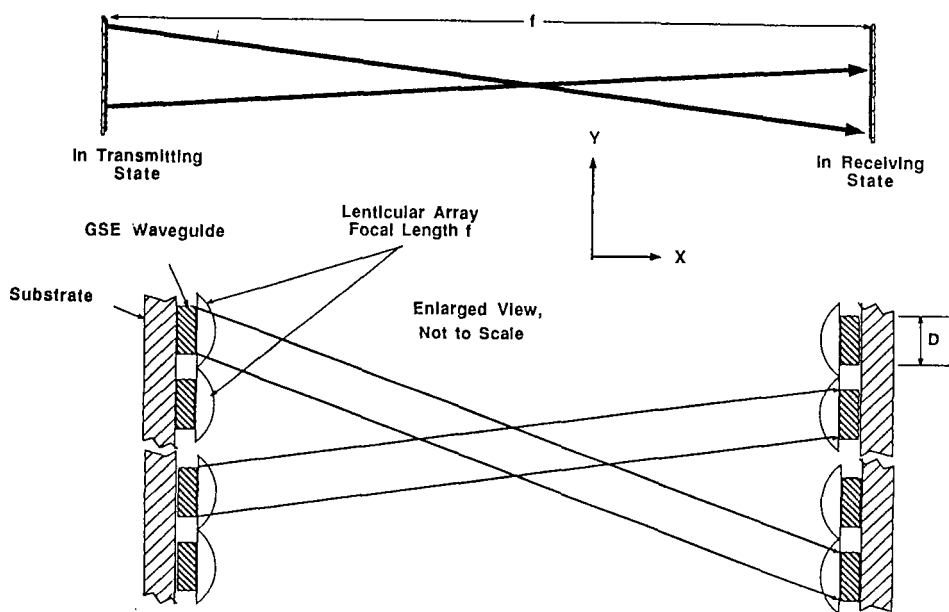


Figure II-3. Schematic of a lenticular lens array of focal length f positioned to couple two GSE-TL arrays together to form a complete backplane interconnect for computer use. The focal length of the lenslets in the lenticular array may be chosen to optimize the optical coupling between the arrays.

In the illustration of Fig. II-3, row N of the transmitting array is deflected through an angle Θ_N and addresses row L of the receiving array. At the same time, row M is deflected through an angle Θ_M and addresses row P of the receiving array. The light leaving each cell may be modulated or switched on and off by addressing the appropriate signal to the quantum-well switch detector (QWSD) of that cell through the switch bus. In the transmitting state, all of the QWSDs will be biased to act as switches. For example, in forward bias, the signal might be used to reverse the polarity across the QWSD causing a strong absorption.

The tunable laser uses short Bragg reflecting gratings that are sufficiently strong to reflect the required amount of light in a relatively short length allowing for a large tuning range. Because of this, we refer to this novel concept as an abrupt DBR tunable laser. The tuning is accomplished by changing the phase length of the composite laser cavity, consisting of a pump section and a tuning section, through current variation [2,3]. A recent article reports wide tuning range in a multi-section DBR laser, with a gain control and an active DBR region where the effective index and, hence, the reflecting wavelength of the Bragg grating is changed by changing the injection current [4].

In our approach, the laser couples directly to a collinear amplified quantum-well (QW) ridge waveguide provided with electrodes so that current pumping can be used to provide just enough gain to cancel out waveguide absorption and scattering losses. Excessive gain in the waveguide might cause loss of resolution and excessive cross-talk due to spontaneous emission. This potential problem requires further study.

The directional couplers connect the amplified ridge waveguide to QW switch-detectors [5,6] that are coupled directly to grating-surface-emitting waveguides [7,8]. The lengths of the directional couplers along a row of cells is varied so that an equal amount of light energy is coupled to each GSE-WG. The last coupler in a row of N is, of course, then chosen to couple all of the remaining light into the Nth GSE-WG. The light transferred by the directional coupler is deflected by Bragg-corner gratings through 90° into wide (W large) waveguides that contain the QW switch-detectors and the surface-emitting gratings. We refer to these waveguides as grating-surface-emitting (GSE) waveguides.

The quantum-well switch-detectors (QWSD) have electrodes and use the QW structure with variable bias. For use in the transmitting state, switching

from reverse to forward bias will give a strong change in absorption to act as a switch or modulator [9,10].

The array acts as an optical receiver as follows: The same GSE waveguides used as output couplers in the transmitting state serve as input couplers in the receiving state. Light falling on such a GSE waveguide at the same angle as that through which it was emitted from a similar GSE waveguide at the transmitting array, will be coupled into the waveguide and flows toward the QWSD. The input coupling fraction will, in theory, be equal to the output coupling fraction of the transmitting grating if the input beam waist is located at the input grating plane and is equal in size to the beam waist at the transmitting grating. The beam waist can be matched in one direction using a lenticular array as shown in Fig. II-3. The focal length of each lenslet is chosen to give the desired beam waist at the receiver. In the receiving state, the QWSD will be placed in reversed bias, and the photocurrent will be brought out to a preamplifier by the detector bus.

We wish to point out that if full duplex operation is required, additional grating waveguides and quantum-well detectors independent of the transmitting GSE waveguides can readily be added to the array. In this case, the same analysis applies and the characteristics, as far as signal to noise, bit error rate, and power requirements described below, will be obtained.

An initial approach utilizing single wavelength lasers connected through Y branches to GSE waveguides was considered early in the program. From our initial considerations, we concluded that the Y branch approach is excessively costly in power loss and requires too great a complexity of laser sources to be practical.

Section III

METHODS OF SCANNING GSE OPTICAL BEAMS

A. RESOLUTION OF ANGULARLY SCANNED OPTICAL BEAMS

It is important to know how much deflection is required so that at the receiver plane a row of GSE waveguides is addressed without crosstalk to the adjacent row. We thus give here a brief review of the resolution of a scanned coherent light beam such as will be emitted from the GSE waveguides.

A wave leaving an aperture D in length, as illustrated in Fig. III-1, comes to a focus at the focal plane of a lens in which it has a beam waist $d = f \cdot \delta\Phi$ caused by the diffraction angle $\delta\Phi$. For a Gaussian beam, the diffraction angle is given by

$$\delta\Phi = \frac{4\lambda}{\pi D} \cong 1.27 \frac{\lambda}{D} \quad (1)$$

If such a beam is deflected through an angle $\delta\Theta$, as illustrated in Fig. III-2, then the number of resolved "spots", N , is just equal to the number of $\delta\Phi$ s contained in the angle $\delta\Theta$ or

$$N = \frac{\delta\Theta}{\delta\Phi} = \frac{\pi D \delta\Theta}{4\lambda} \quad (2)$$

We, thus, see that the number of resolved spots increases directly with the aperture D and the deflection angle $\delta\Theta$.

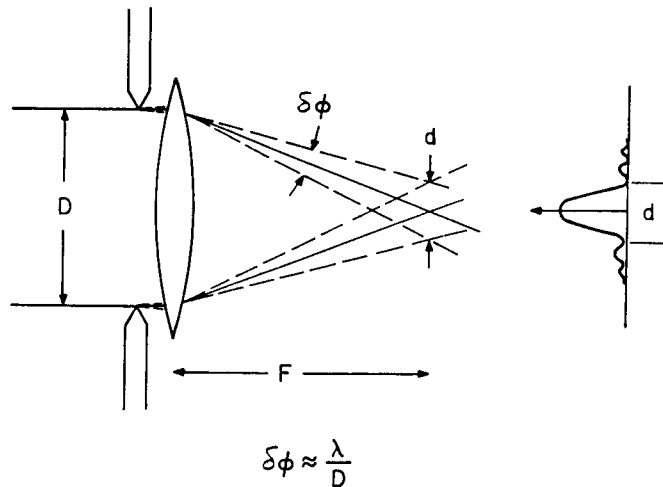


Figure III-1. Illustration of diffraction spreading from aperture.

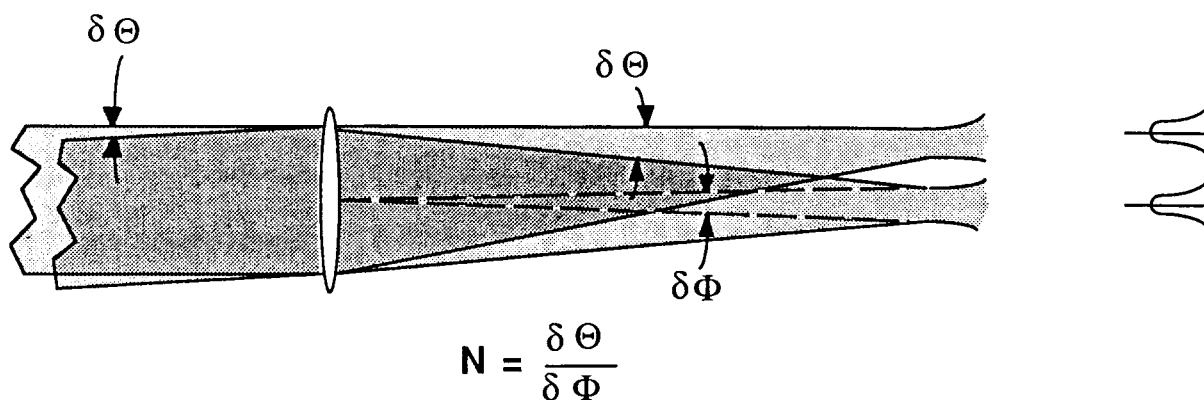


Figure III-2. Illustration of how diffraction effects number of resolved spots.

B. BEAM SCANNING POSSIBILITIES WITH GSE WAVEGUIDES

A schematic cross-section of a GSE waveguide is shown in Fig. III-3.

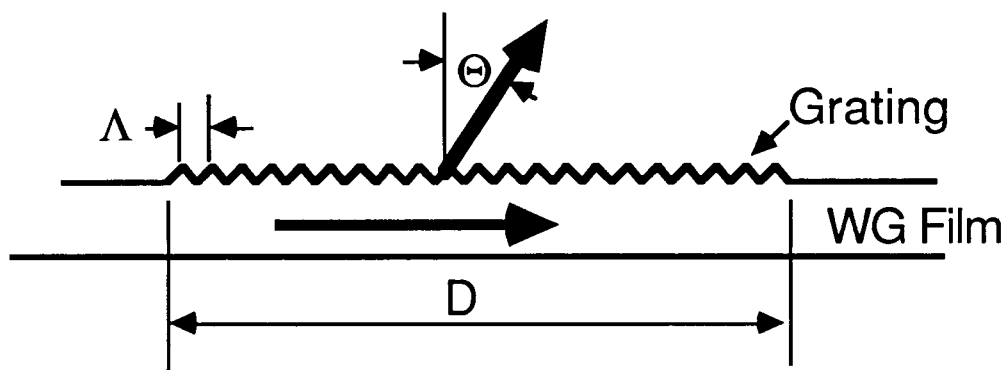


Figure III-3. Schematic of grating-surface-emitting (GSE) waveguide.

Light flowing in the waveguide film is coupled out of the film at an angle Θ to the normal by the grating. The coupling is governed by the following relation:

$$n_0 \sin\Theta = n_e - m_c \lambda / \Lambda \quad (3)$$

n_0 is the refractive index of the space into which the light is coupled, n_e is the effective refractive index of the guided mode, λ is the free space wavelength, and Λ is the grating period. It is clear from Eq. (3) that Θ may be changed by changing the wavelength λ , by changing the effective index of the guided mode, or by changing the grating period Λ .

Consider the case of changing the wavelength. We would like to obtain the relation between the wavelength change and the number of spots (or rows in our

case) that can be resolved. To do this, we take the derivative of Eq. (3) with respect to the wavelength and obtain

$$\delta\Theta = -m_c \frac{\delta\lambda}{\Lambda \cos \Theta}, \quad (4)$$

where $\delta\lambda$ is the wavelength tuning range required. Equating this deflection angle with the angle ($\delta\Phi$) required to resolve one spot from Eq. (3), we obtain

$$\delta\lambda = \frac{4\lambda\Lambda \cos \Theta}{\pi D m_c} \text{ per spot.} \quad (5)$$

By way of an example, take $D = 500 \mu\text{m}$, $\Lambda = 0.25 \mu\text{m}$, and $m_c = 1$ (first order), then $\delta\lambda = 5.27\text{-}\text{\AA}/\text{spot}$. For a 32-row device, the wavelength would be tuned over an approximate range of 169\AA . Wavelength tuning of 1100\AA has already been reported in a DBR diode laser by B. Broberg and S. Nilsson [4]. We will, however, consider the resolution of wavelength addressed GSE waveguides in greater detail in Section IV.

We now consider using a refractive index change such as might be produced by the linear electro-optic (Pockels) effect. To analyze this case, we take the derivative of Eq. (3), with respect to n_e , to find $\delta\theta$ and then, as in Eq. (5) equate this deflection angle with the angle ($\delta\Phi$) required to resolve one spot from Eq. (2) and obtain

$$\delta\Theta = \delta n_e = \frac{4\lambda}{\pi D} \text{ per spot.} \quad (6)$$

Using the same example as before ($D = 500 \mu\text{m}$, $\lambda = 0.83 \mu\text{m}$), we find $\delta n_e = 2 \times 10^{-3}/\text{spot}$. Here, for a 32-row device, an index change of 6.4×10^{-2} would be required. This is far larger than the index changes that are available from practical electro-optic materials. We will, therefore, not consider this approach further in this report.

Finally, we consider changing the angle by changing the period of the grating. On the face of it, this approach might seem unrealizable as we picture the grating as a fixed mechanical structure that might be etched as a surface relief grating on the waveguide. An acoustic wave, however, launched with the propagation vector parallel to the grating vector will result in a composite grating, with a grating period that varies as the acoustic frequency is varied. The effect of such a variation is obtained by taking the derivative of Eq. (3) with respect to the

grating period Λ to find $\delta\theta$ and then again, as in Eq. (5), equating this deflection angle with the angle ($\delta\Phi$) required to resolve one spot from Eq. (2). We, thus, obtain

$$\delta\Theta = \frac{\lambda}{\Lambda^2} \delta\Lambda = \frac{4\lambda}{\pi D} . \text{ Hence}$$

$$\delta\Lambda = \frac{4\Lambda^2}{\pi D m_c} \text{ per spot.}$$

Some details of the calculation of acoustic frequency change required to obtain a given number of resolved spots in this type of approach are given in the Appendix. Based on considerations of structural simplicity, we agreed that further study of the acoustic wave approach was not warranted.

Section IV

WAVELENGTH TUNING RANGE AND RESOLUTION OF GSE-TL APPROACH

A. RESOLUTION OF WAVELENGTH SCANNED GSE

In this section, we give more details on the resolution of a wavelength scanned GSE waveguide. In considering the actual resolution at output coupling angles that are not close to 90° , the effective aperture of the emitting waveguide must be taken into account. We must also consider the effect of the grating order on the resolution. As will be seen, when the effective aperture is taken into account, the resolution is independent of the order but depends on the angle around which the output coupling angles vary as the wavelength is tuned, in addition to the wavelength range and aperture.

Referring to Fig. IV-1, the effective aperture, D_e , is given by

$$D_e = D \cos \Theta. \quad (7)$$

Then the far-field spread [Eq. (1)] becomes

$$\delta\Phi = \frac{4\lambda}{\pi D_e} = \frac{4\lambda}{\pi D \cos \Theta}. \quad (8)$$

To obtain N spots, $\delta\Theta = N\delta\Phi$. Using Eqs. (5) and (8), we obtain that the number of resolved spots (or in our particular case rows) is given by

$$N = \frac{\pi m_c \delta\lambda D}{4n_0 \lambda \Lambda}. \quad (9)$$

From Eq. (1), we find that if we pick a given angle of operation at the center wavelength λ , the grating period is given by

$$\Lambda = \frac{m_c \lambda}{(n_e - n_0 \sin \Theta)}. \quad (10)$$

Substitute Eq. (10) in Eq. (9) then

$$N = \frac{\pi}{4} \left(\frac{n_e}{n_0} - \sin \Theta \right) \frac{D}{\lambda^2} \delta\lambda. \quad (11)$$

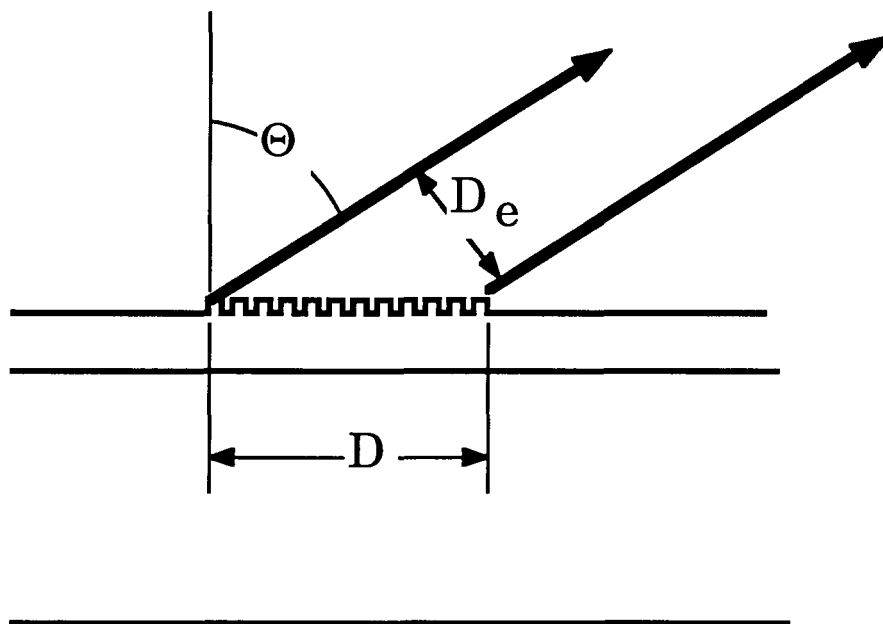


Figure IV-1. Effective aperture, D_e , is less than the aperture D when Θ is not 90° .

It can be seen from Eq. (11) that N depends on the center wavelength, the angle of emission of the center wavelength, the aperture, the refractive indexes, and the wavelength tuning range. N does not depend on the order chosen to give the desired emission angle. This is important in allowing an order and angle to be chosen that will avoid Bragg reflection in the waveguide plane. Such in-plane reflections would introduce losses and will, therefore, be avoided. As is well known, a first-order ($m_c = 1$) grating coupler designed to couple light out perpendicular to the waveguide plane has a second-order grating coupler that reflects light backwards in the waveguide plane. In Fig. IV-2, using Eq. (11), the number of addressable rows is plotted against the output coupling angle when the wavelength is tuned $\pm 100 \text{ \AA}$ around a center value of $0.83 \text{ }\mu\text{m}$. The GSE waveguide grating length is $D = 500 \text{ }\mu\text{m}$, $n_e = 3.4$, and $n_0 = 1$.

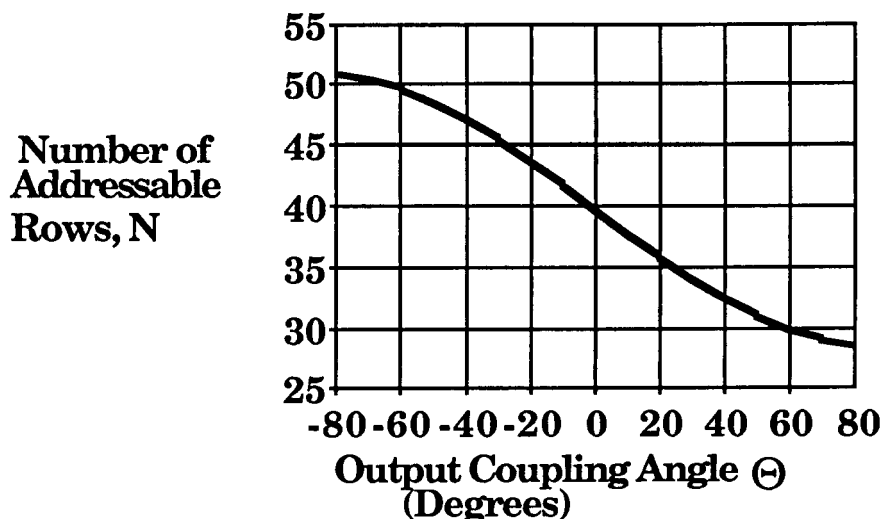


Figure IV-2. Number of addressable rows plotted against the output coupling angle measured from the normal to the waveguide plane when the wavelength is tuned $\pm 100 \text{ \AA}$ around a center value of $0.83 \text{ }\mu\text{m}$. The GSE waveguide grating length is $D = 500 \text{ }\mu\text{m}$, $n_e = 3.4$, and $n_0 = 1$.

As can be seen from Fig. IV-2, more than 40 rows can be addressed at an angle of about -10° (backward from the normal). Angles close enough to the normal to be convenient would be preferred and yet can still be chosen to avoid the problem of second-order Bragg scattering that would occur very close to 0° . In a wavelength range of $\pm 150 \text{ \AA}$, the beam angle swings by $\pm 1.03^\circ$. Thus, it is easy to operate near normal without swinging into the reflection condition at the extrema of the tuning.

B. TUNING ABRUPT DBR; GRATING REQUIREMENTS

There have been a number of reports on the tuning of lasers using current control sections in GaAs quantum-well lasers [2,15,16]. Many of these employed DBR sections [6] tune a multi-section GaAs heterostructure laser and obtain beam deflection from an external waveguide grating section. In addition, tune a GaInAsP/InP DBR laser using a tuning region to tune the cavity length. Most recently, B. Broberg and S. Nilsson [4] report the observation of 11.6 nm (116 \AA) of tuning in a DBR InGaAsP/InP laser with a single gain section. Injected current is used to vary the refractive index of the DBR section. This method would certainly be applicable to OBIT and further enhance the tuning obtainable by using multiple gain sections as we assumed for the present study.

Here we review the grating properties required to allow wide-band tuning of a distributed Bragg reflecting (DBR) laser. As will be seen, very simple considerations show that a grating with a high coupling coefficient for Bragg reflection and short length is required. We refer to wavelength tunable lasers using this "strong" short DBR section as "Abrupt DBR Tunable Lasers."

Figure IV-3 is a simplified view of a cross-section through a GSE waveguide.

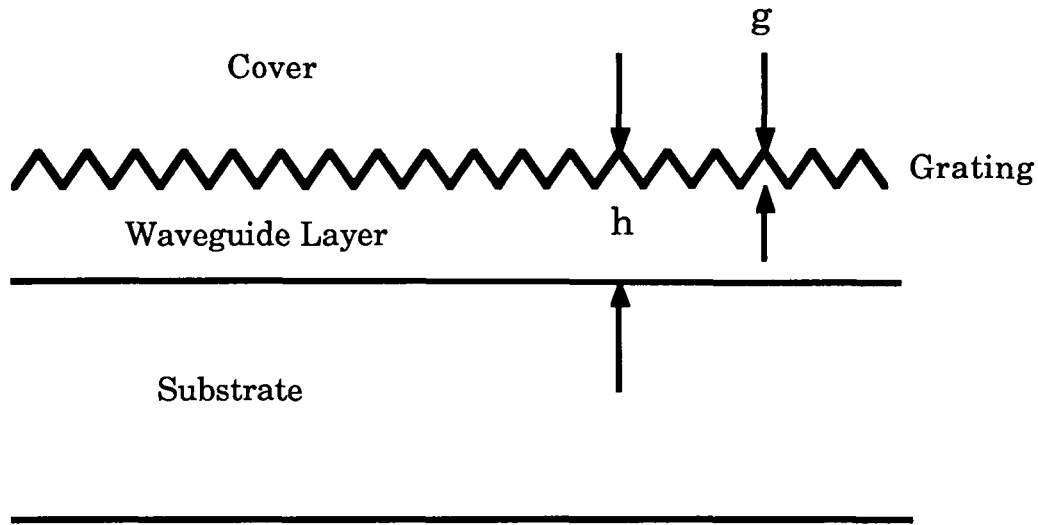


Figure IV-3. Cross-section through a GSE waveguide. The refractive index of the waveguide layer is $n_f = 3.48$. That of the substrate is $n_s = 3.39$. The cover is assumed to be air, with a refractive index $n_c = 1$.

The Bragg reflecting coupling coefficient κ for such a waveguide may be estimated from the following formula [11]:

$$\kappa = \frac{\pi g}{2\lambda} \frac{1}{h + \frac{\lambda}{2\pi} \left(\frac{1}{\sqrt{n_e^2 - n_s^2}} + \frac{1}{\sqrt{n_e^2 - n_c^2}} \right)} \frac{n_f^2 - n_e^2}{n_e} \quad (12)$$

n_f is the refractive index of the waveguide layer, n_s is the refractive index of the substrate, n_c the refractive index of the cover, n_e is the effective refractive index of the guided mode, g is the grating depth, and h is the thickness of the guiding layer. For a coupling coefficient κ and a grating length L , the light intensity reflection coefficient R is given by

$$R = \text{Tanh}^2(\kappa L) \quad (13)$$

The width of the band of wavelengths, in which the reflection remains above a factor of 1/2 from the center value is the reflection linewidth $\Delta\lambda$, may be found from the grating resolution, which equals the number of grating spaces in the aperture

$$\frac{\lambda}{\Delta\lambda} = \frac{L}{\Lambda} \quad \text{whence} \quad \Delta\lambda = \frac{\lambda\Lambda}{L} \quad (14)$$

As is well known, n_e may be found from the dispersion relation for optical waveguides [11]. For a graded index separate confinement heterostructure (GRINSCH) single quantum well (SQW) waveguide in GaAlAs, we calculate the equivalent indexes for use in Eq. (12) to be $n_f = 3.48$, $n_s = 3.39$, and taking $n_c = 1$ (air), the effective index of the guided mode is found to be $n_e = 3.4225$ when the guide thickness is $h = 0.4 \mu\text{m}$. With these values at a wavelength of $0.83 \mu\text{m}$, we find $\kappa = 0.260 \text{ g} (\mu\text{m}^{-1} \text{ for } g \text{ in } \mu\text{m})$. A plot of Bragg reflecting grating length (left ordinate) and grating reflection line width (right ordinate) against grating reflectivity for a grating on the AlGaAs waveguide described above is given in Fig. IV-4. The plot is for a grating depth, g , of $0.1 \mu\text{m}$, which is 25% of the guide thickness' making for a very strong grating. A second-order Bragg grating, with a period of $0.24 \mu\text{m}$, is assumed.

For high-power diode lasers, either output facet or DBR reflectivities below 10% are required for efficient operation. For our assumed conditions, it may be noted from Fig. IV-4 that a 7% reflecting grating will be approximately $10 \mu\text{m}$ long and have a grating reflection linewidth of approximately 200 \AA . This will allow sufficient wavelength tuning to obtain the 32-spot resolution discussed in Section IV, A.

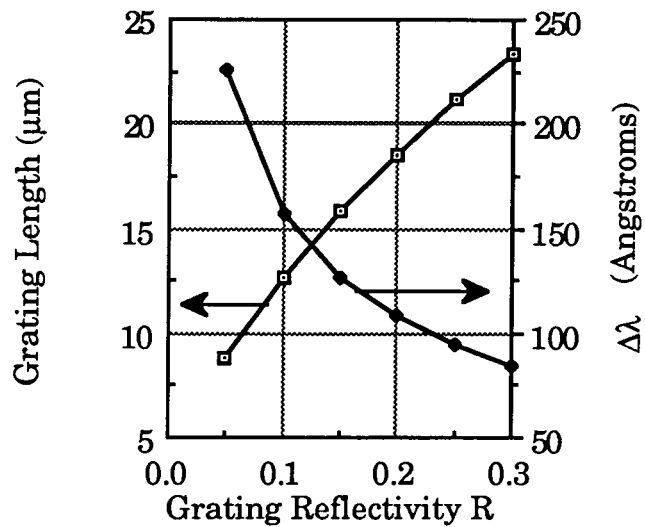


Figure IV-4. Plot of Bragg reflecting grating length (left ordinate) and grating reflection line width $\Delta\lambda$ (right ordinate) against grating reflectivity for a grating on an AlGaAs waveguide. The strong grating has a depth g of $0.1 \mu\text{m}$, which is 25% of the guide thickness.

Section V

POWER REQUIREMENTS AND LOSSES

In this section, we will consider the problem of obtaining sufficient signal intensity at the receiver to ensure that the signal-to-noise ratio (S/N_o) and, hence, bit error rate (BER) is adequate to operate the optical backplane switch as a useful computer tool. A BER of 10^{-9} or better is considered as necessary in most digital communication applications, including those used for interconnecting computers. We will, therefore, use the obtainability of a 10^{-9} BER as a required goal to evaluate the optical backplane approach being considered by this study.

A. RECEIVER POWER NEEDED TO ACHIEVE 10^{-9} BER

For most, if not all, coding schemes a conservative estimate of the required received signal-to-noise ratio is $S/N_o = 25$ dB. We will now calculate the S/N_o ratio as a function of received power. We consider that an array unit cell acting as a receiver may be represented by the equivalent circuit shown in Fig. V-1.

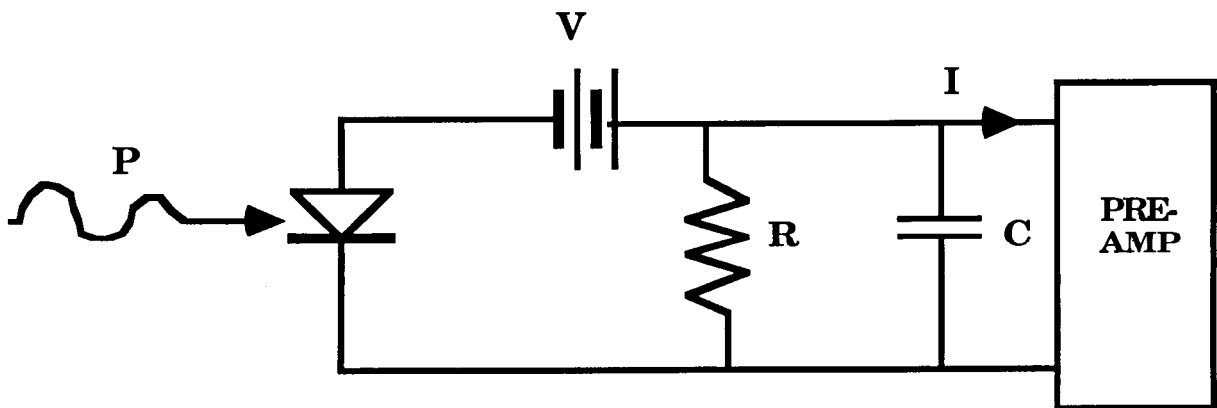


Figure V-1. Equivalent circuit representation of a unit cell of an OBIT array operated in the receiving mode.

In the equivalent circuit of Fig. V-1, the quantum well switch detector (QWSD) section of each unit cell is represented by a junction detector back-biased with a suitable voltage V through the detector bus that electrically connects the QWSD and the input resistor of a pre-amplifier. The effective input impedance of the pre-amp is considered to be represented by a resistor R shunted by a

capacitor C. The optical power actually arriving at the QWSD is P. The RMS signal (power) arriving at the pre-amp is then given by

$$S = \frac{1}{2} I^2 R = \frac{1}{2} \left(\eta \frac{e\lambda}{hc} \right)^2 P^2 R \quad (15)$$

η is the quantum efficiency of the QWSD, e is the charge on an electron, and hc/λ is the photon energy in which h is Plank's constant and c is the velocity. The RMS noise power, N_s , is given by [12].

$N_s = \text{shot noise } (2eI \Delta f R) + \text{Johnson (thermal) noise } (4kT\Delta f)$

$$N_s = \left\{ 2 \left(\eta \frac{e\lambda}{hc} \right) e P + \frac{4kT F}{R} \right\} \Delta f R \quad (16)$$

k is Boltzman's constant. The pre-amp load resistance is $R = 1/(2\pi \Delta f C)$. The bandwidth is Δf , the pre-amp noise figure is F , and the input temperature is T . As an example, consider a future, very fast computer requiring bandwidth $\Delta f = 100$ MHz. Assume $F = 2$, $\eta = 0.5$, $C = 100$ pF, and $\lambda = 0.83$ μm . We then calculate that the required optical power entering the QWSD to obtain $S/N = 25$ dB and 10^{-9} BER is

$$P = 1.12 \text{ mW.}$$

B. SYSTEM LOSSES

Having calculated the required power at the receiver, we now must find the losses in the system in order to find out how much power is required from the lasers. We will separately consider losses within the transmitting array, losses that occur as part of the transmission, and losses that occur within the receiving array.

1. Losses in the Transmitting GSE-TL Array

In the GSE-TL approach, we are considering that the light from each laser is divided among all the N unit cells of a row. The amplified QW ridge waveguide is assumed to have only enough gain to compensate for the absorption and scattering losses of the waveguide thus, the power division loss is not compensated by the gain. This assumption is made because having enough gain to compensate for the power division appears likely to introduce enough

incoherent light to prevent the array from operating correctly. We, thus, take the power division loss to be simply $1/N$.

We assumed earlier that the directional couplers along one row would have coupling lengths graded so that each GSE waveguide of a transmitting row would receive the same amount of light. The lengths required to give the correct division at the center wavelength are calculated below. As the wavelength is tuned, however, the division of light among the couplers will no longer be equal, and this effect must be considered the same as a loss. As will be seen in the calculation below, the effect, fortunately, turns out to be rather small.

We first calculate the directional coupler lengths required for an equal division of light power among the N GSE waveguides of a row. Going from the laser, each successive "downstream" coupling length must be longer than the preceding one to compensate for the diminished available light. If the input light power is P_0 and there are N couplers, each coupler must extract light power equal to P_0/N . The coupling fraction of a directional coupler of length L_n is $\sin^2(\kappa_c L_n)$. κ_c is the coupling coefficient. We write a sequence starting with the first directional coupler (subscript 1) and going to the n 'th coupler (subscript n). The sequence makes the required relation clear.

$$\begin{aligned}
 P_1 &= P_0/N = P_0 \sin^2(\kappa_c L_1) \\
 P_2 &= P_0/N = (P_0 - P_0/N) \sin^2(\kappa_c L_2) \\
 P_3 &= P_0/N = (P_0 - 2P_0/N) \sin^2(\kappa_c L_3) \\
 &\dots \\
 P_n &= P_0/N = [P_0 - (n-1)P_0/N] \sin^2(\kappa_c L_n)
 \end{aligned} \tag{17}$$

We now need only invert Eq. (17) to find the required coupling length for the n 'th directional coupler. Thus,

$$L_n = \frac{1}{\kappa_c} \sin^{-1} \sqrt{\frac{1}{N - n + 1}} \tag{18}$$

The coupling lengths calculated using Eq. (18) will distribute the light equally at the center wavelength. As the wavelength is tuned, the coupling coefficient will change, and the lengths will not be correct for equal power distribution. Thus, some channels will have less light than others, and the effect of this reduction is the same as the effect of any other loss. To calculate the

magnitude of this source of loss, we will write the expression for the coupling coefficient of directional couplers and then take its derivative with respect to wavelength. From the variation of the coupling coefficient with wavelength, we can calculate the resulting change in the power coupled or transmitted by the n'th coupler. We then plot the change in transmission as a function of coupler number to evaluate the effect.

Figure V-2 is a cross-section through a directional coupler consisting of two identical, dielectric waveguides each W wide spaced a distance D apart. D is small enough so that the evanescent fields of the two guides overlap. The guides run parallel to each other normal to the x-y plane of the paper. The rectangular guides have a refractive index n_f that is greater than the refractive index n_s of the substrate or cladding in which they are embedded. For such guides that may be used to represent the ridge guides of this study by correctly choosing the indexes, the coupling coefficient is given to a good approximation by [13]

$$\kappa_c = \frac{2(n_f^2 - n_e^2)\sqrt{n_e^2 - n_s^2}}{Wn_e(n_f^2 - n_s^2)} \exp \frac{2\pi}{\lambda} \sqrt{n_e^2 - n_s^2} D \quad (19)$$

n_e is the effective index of the guided mode of an isolated rectangular guide.

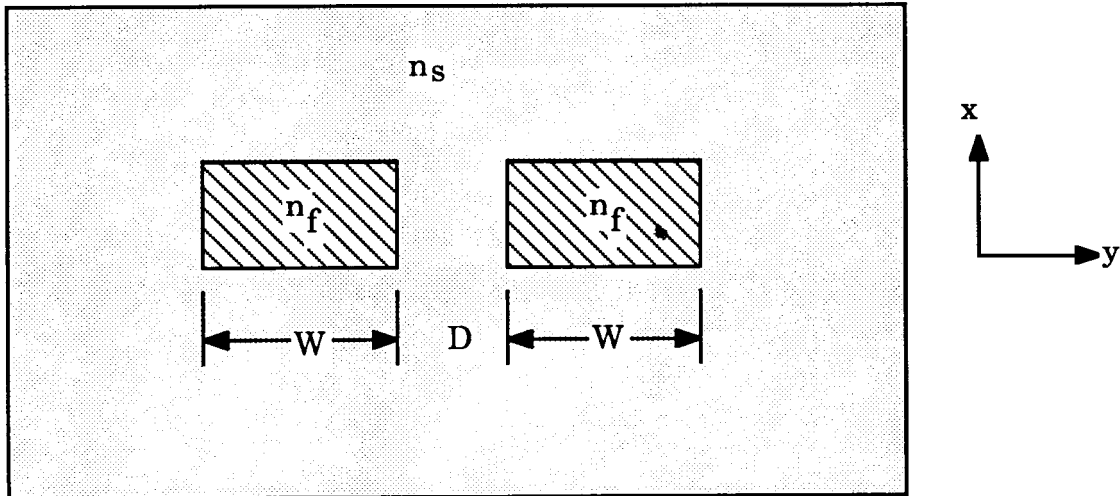


Figure V-2. Directional coupler consisting of two identical rectangular dielectric waveguides of refractive index n_f embedded in a substrate of lower refractive index n_s .

The coupling coefficient varies with wavelength, and the power transferred by the directional couplers varies with the coupling coefficient. We first calculate

the variation of κ_c with λ including the dispersion in the refractive indexes. Taking the derivatives, we find, after some manipulation,

$$\frac{d\kappa_c}{\kappa_c} = -\frac{2\pi D}{\lambda^2} \sqrt{n_e^2 - n_s^2} \delta\lambda + \left\{ 2 \frac{n_f - n_e}{n_f^2 - n_e^2} + \frac{n_e - n_s}{n_e^2 - n_s^2} - 2 \frac{n_f - n_e}{n_f^2 - n_s^2} - \frac{1}{n_e} + \frac{2\pi D(n_e - n_s)}{\lambda \sqrt{n_e^2 - n_s^2}} \right\} \frac{dn}{d\lambda} \delta\lambda \quad (20)$$

To complete our task, we calculate how the power coupled by the n 'th coupler varies with the coupling coefficient. Taking the derivative of Eq. (17), with respect to κ_c , we obtain the normalized transmission variation in P_n .

$$1 - \frac{\delta P_n}{P_n} = 1 - \frac{2 \sin^{-1} \sqrt{\frac{1}{N-n+1}}}{\tan\left(\sin^{-1} \sqrt{\frac{1}{N-n+1}}\right) \kappa_c} \frac{d\kappa_c}{\kappa_c} \quad (21)$$

Using the values of refractive indexes given in Section IV, B and, as there taking $dn/d\lambda = -0.1/\mu\text{m}$, in Fig. V-3 we plot the normalized transmission as a function of n using Eqs. (20) and (21). The wavelength variation is, as before, 200 \AA , and we assume a 32-bit GSE-TL array so that $N = 32$.

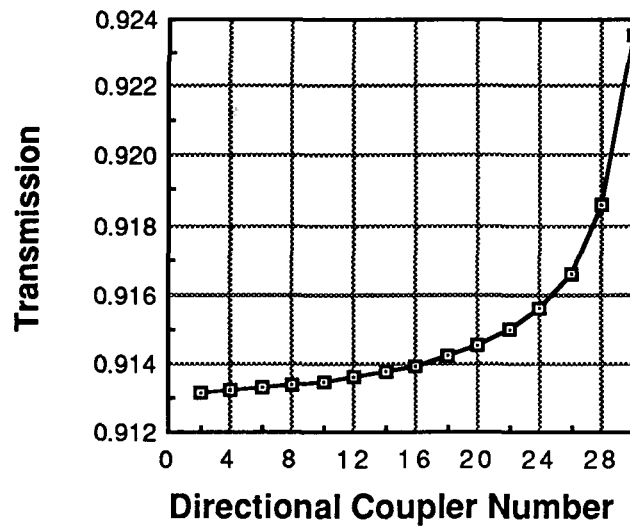


Figure V-3. Variation of transmission from waveguide to GSE grating with directional coupler number for $\delta\lambda = 200 \text{ \AA}$.

As can be seen from Fig. V-3, the change in transmission is relatively small falling to about 0.9 (90%) of its maximum value for the most sensitive coupler at the tuning extreme. The first coupler is the shortest and, thus, suffers the strongest effect when the wavelength is scanned to its maximum excursion. It can be concluded that the effect of wavelength tuning on the directional couplers will not seriously impair the operation of the GSE-TL array. The 10% loss will, however, be included in the power budget.

We now discuss the losses that occur in the output grating coupling process. The grating depth and, hence, coupling coefficient can readily be made strong enough to couple all the light out of the waveguide in the 500- μm grating length allotted. Experience at the David Sarnoff Research Center has shown that gratings with depths under 1000 \AA remove all the light from the waveguide in lengths less than this value. The exact depth required may be calculated from computer programs available at the David Sarnoff Research Center. The problem is, however, that the light is coupled out in both directions to the waveguide plane. Thus, the light coupled in the "wrong" direction is lost. We will assume a worst case and choose the direction for output coupling to be away from the substrate. That is, we will assume that the GSE-TL array is not grown on a transparent substrate. We have observed that without blazing or other measures being taken, the ratio of light grating-coupled from a waveguide to a cap layer to the light coupled to the substrate, is roughly equal to the ratio of their refractive indexes. Thus, we will take the worst-case loss as resulting in a transmission of $1/n_s$ at the output grating coupler.

The loss at the transition from the abrupt DBR tunable laser to the amplified QW ridge waveguide is expected to be negligible as the waveguide will be identical in structure to the laser section. The waveguide is distinguished from the laser section by having an independent pumping electrode. The losses in the transmitting GSE-TL array are summarized as follows:

	<u>Transmission</u>
Power Division	$1/N$
Directional Coupler	0.9 worst case for $N = 32$
Output grating Coupler	$1/n_s$

The actual values used for these are listed in Table V-1 below.

Table V-1
OPTICAL LOSSES

Transmitter	
Power division among N GSE waveguides	1/N
Abrupt DBR laser-WG coupling	1.0
Directional coupler	0.9
Output grating coupler	1/n _s
Receiver	
(Beam waist matched to output grating in Y direction)	
Input grating coupler	1/n _s
Mismatched beam waist in Z direction (W _r /W ≠ 1)	(W/D) ²
Total Optical Loss	$\frac{0.9W^2}{N n_s^2 D^2}$

Example: For a monolithic AlGaAs, 32 x 32 optical backplane interconnect, N = 32. Substrate refractive index, n_s = 3.4. GSE waveguide length is D = 500 μm and width W = 100 μm.

$$\text{Total Optical Loss} = 9.7 \times 10^{-5} \text{ (40 dB)}$$

2. Transmission and Input Grating Coupling Losses

Light leaving a GSE waveguide of a GSE-TL array in the transmitting state passes through a lenslet of the lenticular array associated with the transmitter. The lenticular array is placed sufficiently close to the surface of the GSE-TL wafer as to be considered in substantial contact with the surface. The light passes through air and is received by a lenslet of the identical lenticular array associated with the GSE-TL array in the receiving state. The received light is coupled into the receiving array by its GSE waveguide, as will be discussed further below. The arrays are spaced a distance apart equal to the focal length of a lenslet of the lenticular array. For the purpose of this loss estimate, we will consider that the lenticular arrays consist of cylindrical lenslets with axes perpendicular to the x-y plane in which the light is deflected (see Figs. II-3 and V-4) In this case, the

beam waist in the y direction of a transmitted light beam is transferred to the receiver where it has a y dimension given by

$$D_r = f \Delta\Phi \quad (22)$$

f is the focal length of a cylindrical lenslet of the lenticular array, and $\Delta\Phi$ is the diffraction spread of the emitted beam given by Eq. (1). Using Eq. (1) in Eq. (22) and solving for f, we find

$$f = \frac{\pi D D_r}{4\lambda} \quad (23)$$

Since the receiving grating has the same structure and dimensions as the transmitting grating, the input coupling will be optimized in the y direction if the received beam waist in that direction is equal to the y beam waist at the transmitting grating [14]. Thus, setting D_r equal to D in Eq. (23), we find

$$f = \frac{\pi D^2}{4\lambda} \quad (24)$$

For the case we have been taking as an example, f is calculated to be 23.7 cm, which is a reasonable dimension for a lenticular lenslet.

Referring again to Fig. V-4, if we match the beam waist in the y direction, the beam waist in the z direction will not be the same size as the grating width and there will be a geometric loss. That is $W_r \neq W$. Applying Eqs. (22) and (1) and to the z direction, it is readily shown that the ratio of received beam waist width to the transmitted width is given by

$$W_r/W = W^2/D^2 \quad (25)$$

The transmission fraction due to the z direction size mismatch is given by Eq. (25).

We will assume that the lenticular arrays are anti-reflection coated so that there will be no Fresnel reflection loss. Then the only loss during transmission will occur because of size mismatch in the beam widths in the x direction.

The input-grating coupling loss will be equal to the output-grating coupling loss because the beam waist size in the y direction (normal to the grating lines) is matched to that of the input [14]. Thus, as explained in Section V, B-1, the input coupling loss will also result in a transmission of $1/n_s$. Using these equations and considerations, we summarize the total optical losses in Table V-1.

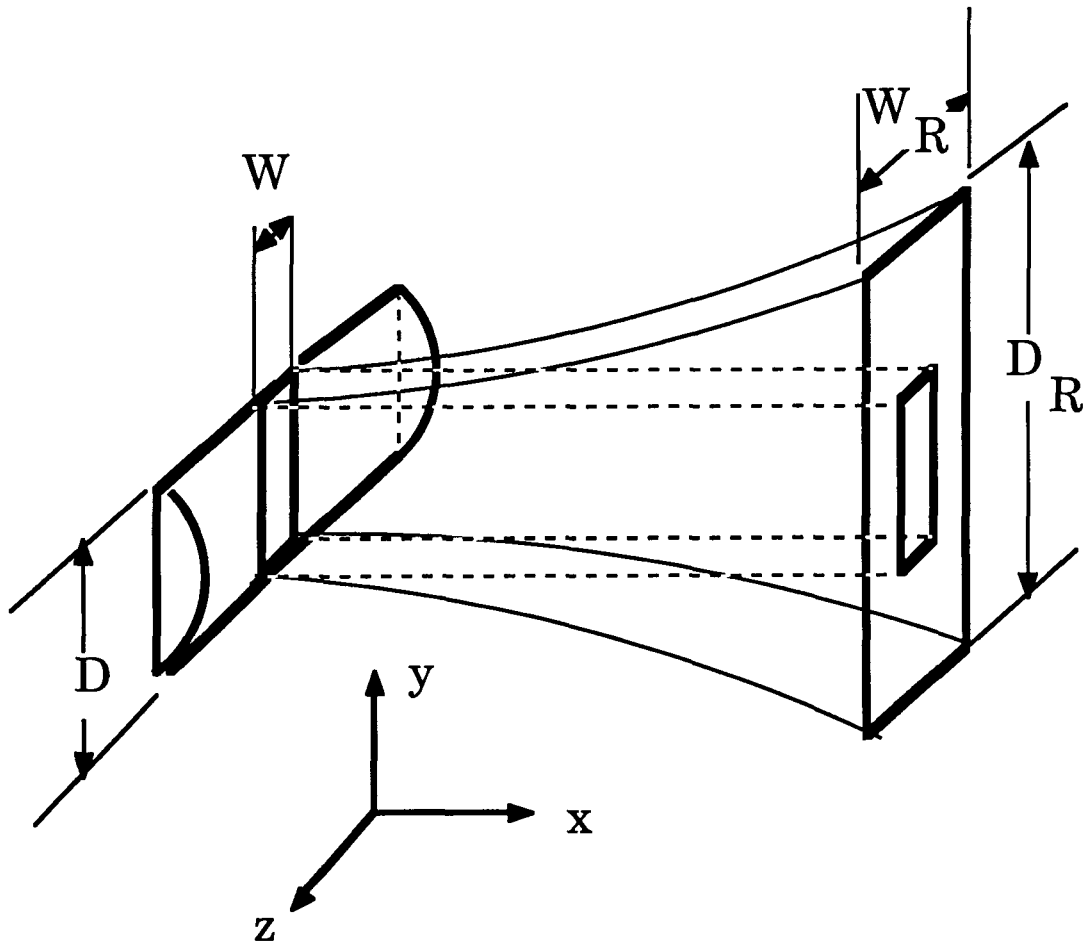


Figure V-4. Perspective view of geometry for calculating coupling between two GSE-TL arrays.

C. SUMMARY OF OPTICAL LOSSES

Using the value of loss summarized in Table V-1 and the optical power required to obtain a BER of 10^{-9} calculated in Section V, A we find the necessary laser power to be

$$\text{laser power for } 10^{-9} \text{ BER} = 1.12 \times 10^{-6} / 9.7 \times 10^{-5} \approx 12 \text{ mW.}$$

In our treatment of loss and power requirements, we have assumed that the arrays and optics can be arranged to avoid crosstalk between separate channels. This assumption should be verified in future work. If crosstalk cannot, in fact be avoided, then additional measures would have to be taken in compensation.

Section VI

CONCLUSION

We may summarize our conclusions as follows: Using our approach employing monolithic, grating-surface-emitting (GSE) waveguides coupled to abrupt DBR or other tunable laser (TL) configurations it should be possible within the present state of the art to have an optical backplane array with the following characteristics:

- Any row of a 32 x 32 GSE array may be optically connected to any row of a second 32 x 32 array.
- By scanning the laser driver of a row of the transmitting array through a wavelength range of 200 Å, any of 32 rows of the receiving array can be addressed.
- Each monolithic array can be used as both transmitter and receiver by switching the bias on the quantum-well switch detectors.
- Separate transmitting and receiving structures could be provided, if desired, for duplex operation.
- For a bit error rate of 10^{-9} at 100-MHz data rate, a required laser power of 12 mW is calculated based on an estimated total optical loss of 40 dB (9.7×10^{-5}).

The advantages of this approach to OBIT are as follows:

- Provides an optical approach to overcome complexity inherent in electronic switching for computer applications.
- Employs and monolithically integrates waveguide and laser diode devices that have been demonstrated. It, thus, does not require the invention of new devices.
- Because a complete backplane array may be formed monolithically on a chip, our approach will be compact and power efficient.

- It should be possible to demonstrate optical backplane switches as large as 32 x 32 using state-of-the-art technology.
- The optical backplane technology studied in this report requires only one switch decision to switch 32 parallel connections to anyone of 32 positions.
- The laser power required to achieve a high level of performance (32 parallel connections to any of 32 positions with 10^{-9} BER at a 100-MHz data rate) is modest for certain types of quantum-well lasers.

There are areas that require further study before the development of a full-scale GSE-TL optical backplane occurs. The tuning range, stability, and repeatability of the tuned laser has to be established. An important element in our approach is the amplified QW ridge waveguide that carries the light from the tuned DBR laser to the grating waveguide via the directional couplers. The effect of the amplified spontaneous emission in the amplified waveguide on the cross-talk and, hence, the required size of the arrays should be studied further. The feasibility of fabricating the required integrated optics' structures has to be evaluated with respect to the required tolerances. Finally, the actual materials integration technology has to be chosen and evaluated. We feel that these important areas can best be addressed through experimental demonstration and studies.

Section VII

REFERENCES

1. T. Tamir, "Beam and Waveguide Couplers," in Integrated Optics, Chapter 3, edited by T. Tamir, 2nd Ed. (Springer Verlag, Berlin), 1982.
2. Y. Tokuda, Y. Abe, T. Matsui, N. Tsukada, and T. Nakayama, "Dual-Wavelength Emission from a Twin-Stripe, Single Quantum-Well Laser," *Appl. Phys. Lett.* **51**, 1664 (23 Nov 87); Y. Tokuda, N. Tsukada, F. Fujiwara, K. Hamanaka, and T. Nakayama, "Widely Separate Wavelength Switching of Single Quantum-Well Laser Diode by Injection Current Control," *Appl. Phys. Lett.* **49**, 1629 (15 Dec 86).
3. H. Imai, Y. Kotaki, M. Matsuda, Y. Kuwahara, and H. Ishikawa, "Wavelength Tunable Laser with Wide Tuning Range," Paper MB1, Conference on Lasers and Electro-Optics (CLEO), Anaheim, CA (April 1988); Y. Kotaki, M. Matsuda, M. Yano, H. Ishikawa, and H. Imai, "1.55- μ m Wavelength Tunable FBH-DFB Laser," *Electron. Lett.* **23**, 325 (1987).
4. B. Broberg and S. Nilsson, "Widely Tunable Bragg Reflector Integrated Lasers in InGaAsP-InP," *Appl. Phys. Lett.* **52**, 1285 (18 April 88)
5. D. A. B. Miller, J. E. Henry, A. C. Gossard, and J. H. English, "Integrated Quantum Well Self-electro-optic Effect Device: 2 x 2 Array of Optically Bistable Switches," *Appl. Phys. Lett.* **49**, 821 (29 Sept 86)
6. Y. Kan, H. Nagai, and M. Yamanishi, "Field Effects on the Refractive Index and Absorption Coefficient in AlGaAs Quantum-Well Structures and Their Feasibility for Electro-optic Device Applications," *IEEE J. Quantum Electron.* **QE-23**, 2167 (12 Dec 87)
7. G. A. Evans, J. M. Hammer, N. W. Carlson, F. R. Elia, E. A. James, and J. B. Kirk, "Surface Emitting Second-Order Distributed Bragg Reflector Laser with Dynamic Wavelength Stabilization and Far-Field Angle of 0.25°," *Appl. Phys. Lett.* **49**, 314 (11 Aug 86).
8. J. M. Hammer, N. W. Carlson, G. A. Evans, M. Lurie, S. L. Palfrey, C. J. Kaiser, M. G. Harvey, E. A. James, J. B. Kirk, and F. R. Elia, "Phase-

- Locked Operation of Coupled Pairs of Grating-Surface-Emitting Diode Lasers," *Appl. Phys. Lett.* **50**, 659 (16 March 87).
9. T. E. Van Eck, P. Chu, W. S. C. Chang, and H. H. Wieder, "Electro-absorption in an InGaAs/GaAs Strained Layer Multiple Quantum-Well Structure," *Appl. Phys. Lett.* **49**, 135 (21 July 86).
 10. D. Ahn and S-L. Chuang, "Calculation of Linear and Nonlinear Inter-sub-band Optical Absorptions in a Quantum-Well Model with an Applied Electric Field," *IEEE J. Quantum Electron.* **QE-23**, 2196 (12 Dec 87).
 11. H. Kogelnik, "Theory of Dielectric Waveguides," in *Integrated Optics*, Chapter 2, edited by T. Tamir, 2nd Ed. (Springer Verlag, Berlin), 1982, pg.75.
 12. S. D. Personick, "Receiver Design for Digital Fiber-Optic Communication Systems, I" *Bell System Technical Journal* **52**, 843-886 (July-August 1973).
 13. See for example R. G. Hunsperger, "Integrated Optics: Theory and Technology," Springer-Verlag, Berlin, 1982, pg 113.
 14. T. Tamir, "Beam and Waveguide Couplers," in *Integrated Optics*, Chapter 3, edited by T. Tamir, 2nd Ed. (Springer Verlag, Berlin), 1982, pp. 110-112.
 15. M. Mittelstein, Y Arakawa, A. Larsson, and A Yariv, "Second Quantized State Lasing of a Current Pumped Single Quantum-Well Laser," *Appl. Phys. Lett.* **49**, 1689 (22 Dec 86).
 16. J. E. Epler, N. Holonyak, Jr., R. D. Burnham, C. Lindstrom, W. Streifer, and T. L. Paoli, "Broadband Tuning ($\Delta E \cong 100$ meV) of $Al_xGa_{1-x}As$ Quantum-Well Heterostructure Lasers with an External Grating," *Appl. Phys. Lett.* **43**, 740 (15 Oct 83).
 17. Y. Tohmori, Y. Suematsu, H. Tsushima, and S. Arai, "Wavelength Tuning of GaInAsP/InP Integrated Laser with Butt-Jointed Built-in Distributed Bragg Reflector," *Electron. Lett.* **19**, 656 (18 Aug 83).

APPENDIX

Scanning of light from a GSE waveguide by varying the grating period using an acoustic surface wave.

The k vector for the coupling grating is $k = \frac{2\pi}{\Lambda}$, that for an acoustic wave launched with k vector parallel to that of the grating is

$$k_A = \frac{2\pi}{\Lambda_A} = \frac{2\pi f}{v_A} \quad (\text{A1})$$

Here v_A is the acoustic velocity, and f is the acoustic frequency. The combined k vector for the acoustic and coupling gratings is

$$k_T = \frac{2\pi}{\Lambda_T}$$

Use

$$k_T = k + k_A.$$

Then

$$\begin{aligned} \delta\Lambda &= |\Lambda - \Lambda_T| = \Lambda \left(\frac{\Lambda_A}{\Lambda + \Lambda_A} \right) - 1 \\ &= N \frac{4\lambda}{\pi D} \text{ for } N \text{ spots} \end{aligned} \quad (\text{A2})$$

From (A1) and (A2), the acoustic frequency range required to resolve N spots is

$$f = \frac{v_A}{\Lambda + \frac{\pi D}{4N}}$$

Plots of the required acoustic frequency tuning range *vs* the length of the Bragg grating for resolution of 8, 16, 24, and 32 spots are given in Fig. A1 for longitudinal acoustic waves in GaAs and, in Fig. A2, for transverse acoustic waves.

Acoustic Frequency vs Bragg Grating Length
GaAs Longitudinal waves, $v=5.15 \text{ E5 cm/sec}$

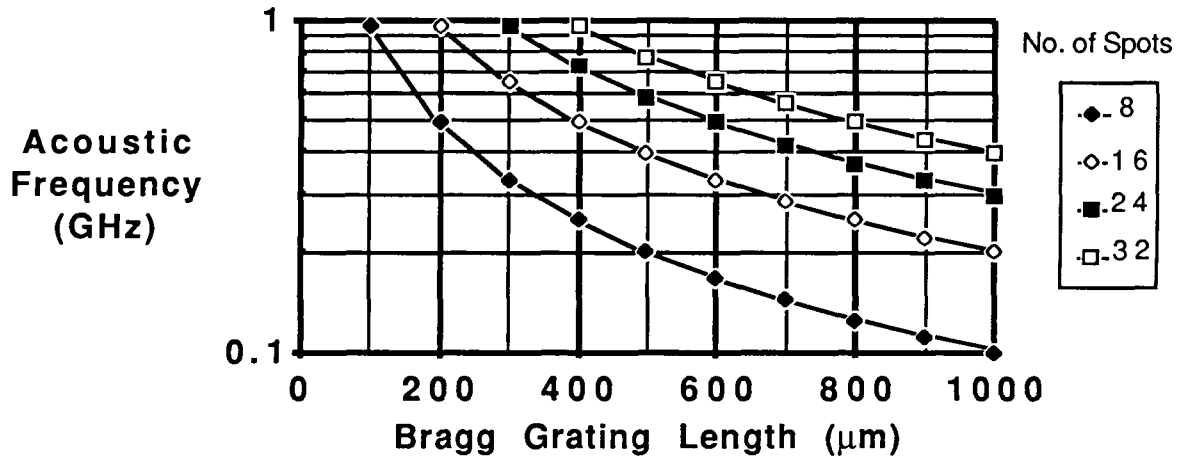


Figure A-1. Acoustic frequency tuning range plotted against length of Bragg grating to obtain 8, 16, 24, and 32 resolved spots, longitudinal [110] acoustic waves in GaAs with wave velocity $v = 5.15 \times 10^5$ cm/sec.

Acoustic Frequency vs Bragg Grating Length

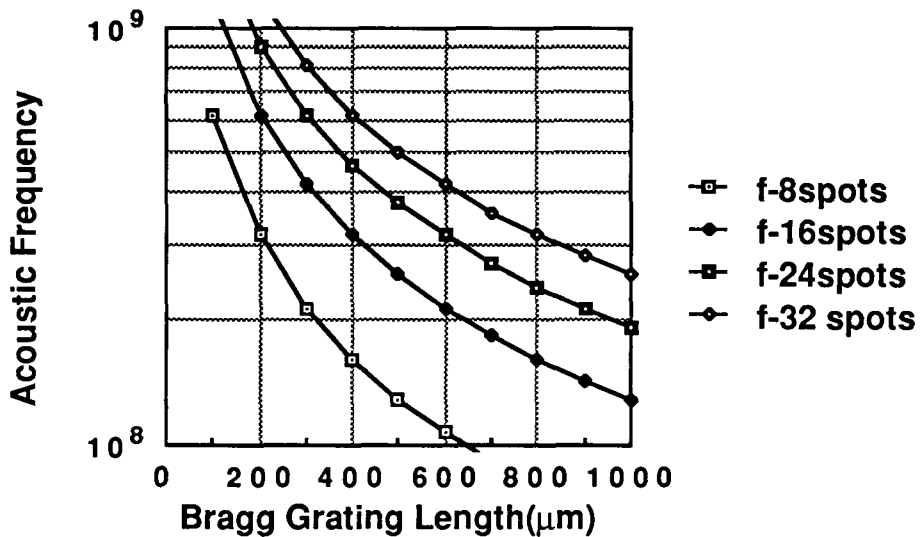


Figure A-2. Acoustic frequency tuning range plotted against length of Bragg grating to obtain 8, 16, 24, and 32 resolved spots, transverse [100] acoustic waves in GaAs with wave velocity $v = 3.32 \times 10^5$ cm/sec.



Report Documentation Page

1. Report No. NASA CR-4209		2. Government Accession No.		3. Recipient's Catalog No.	
4. Title and Subtitle Optical Backplane Interconnect Technology (OBIT)			5. Report Date December 1988		
			6. Performing Organization Code		
7. Author(s) J. M. Hammer			8. Performing Organization Report No.		
			10. Work Unit No. 506-44-21-01		
9. Performing Organization Name and Address David Sarnoff Research Center Princeton, NJ 08543-5300			11. Contract or Grant No. NAS1-18226		
			13. Type of Report and Period Covered Contractor Report 8/24/87 to 3/23/88		
12. Sponsoring Agency Name and Address National Aeronautics & Space Administration Langley Research Center Hampton, Virginia 23665-5225			14. Sponsoring Agency Code		
			15. Supplementary Notes Langley Technical Monitor: Herbert D. Hendricks		
16. Abstract <p>We describe and analyze a novel approach to implementing an Optical Backplane Interconnect Technology (OBIT) that is capable of optically connecting any row of a 32 x 32 backplane array to any row of a second 32 x 32 array. Each backplane array is formed monolithically on a wafer. The technology is based on the use of Grating-Surface-Emitting (GSE) waveguides that are formed on a wafer containing quantum-well and separate confinement waveguide layers. These layers are used for transverse guiding, gain, modulation, detection, and for the formation of wavelength tunable distributed-Bragg reflector lasers. The required surface structures are formed photolithographically. The GSE waveguides act as efficient antennae that radiate light at angles selected by tuning the wavelength of the lasers. The same waveguides may be used as the receiving antennae when the array is used in the receiving mode. Thus, wavelength tuning is used to direct each row of the transmitting array to the desired row of the receiving array. In summary: The optical backplane array will have the following characteristics:</p> <p>Any row of a 32 x 32 GSE array may be optically connected to any row of a second 32 x 32 array. Only one switch decision is required to switch 32 parallel connections to any one of 32 positions</p> <p>Each monolithic array can be used as both transmitter and receiver by switching the bias on the quantum-well switch-detectors.</p> <p>Separate transmitting and receiving structures could be provided for duplex operation.</p> <p>For a bit error rate of 10^{-9} at 100-MHz data rate, a required laser power of 12 mW is calculated based on an estimated total optical loss of 40 dB.</p>					
17. Key Words (Suggested by Author(s)) optical computing optical computer interconnects grating-surface-emitters			18. Distribution Statement Unclassified - Unlimited Subject Category 36		
19. Security Classif. (of this report) Unclassified		20. Security Classif. (of this page) Unclassified		21. No. of pages 44	22. Price A03